Inorganic Chemistry

Article

pubs.acs.org/IC

Ionothermal Synthesis and Structure of a New Layered Zirconium Phosphate

Stef Smeets,[†] Lei Liu,*[,‡] Jinxiang Dong,[‡] and Lynne B. McCusker*[,†]

[†]Laboratory of Crystallography, ETH Zurich, CH-8093 Zurich, Switzerland

[‡]Research Institute of Special Chemicals, Taiyuan University of Technology, Taiyuan 030024, Shanxi, P.R. China

Supporting Information

ABSTRACT: A new layered zirconium phosphate material has been synthesized ionothermally using *N*-ethylpyridinium (Epy) bromide as both the solvent and the template, and its structure has been solved from synchrotron X-ray powder diffraction data using the charge-flipping routine implemented in Superflip. Rietveld refinement coupled with difference electron density map analysis was used to locate the organic cations between the layers. In the final stages of refinement, it became clear that not only ethylpyridinium but also pyridinium ions were present between the zirconium phosphate layers. These findings were then corroborated using elemental analysis, TGA, and solid-state ^{13}C CP/MAS NMR data.

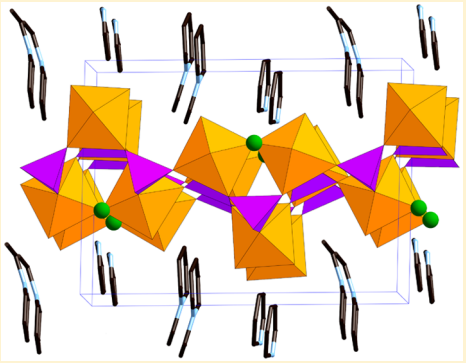

INTRODUCTION

Zirconium phosphate materials have been investigated extensively in view of their potential applications in the fields of catalysis, ion-exchange, gas adsorption/separation, and proton ion conductivity.[1−3] In recent years, efforts have focused on the discovery of new materials with novel structures.[4−8] Most of these materials have been synthesized using a hydro-/solvothermal approach in the presence of organic amines, wherein both the solvent and the organic amines appear to play a key role in determining the structure adopted by the final zirconium phosphate phase.

Ionothermal synthesis is an emerging approach for synthesizing zeolite analogs and other porous solids that was first reported by Morris in 2004.[9] In such syntheses, the ionic liquids or deep eutectic mixtures are used as both the solvent and the template. The pure ionic environment can change the crystallization process and thereby provide new opportunities for the synthesis of novel porous solids.[10,11] For example, ionothermal synthesis produced a layered cobalt aluminophosphate, SIZ-13, with Co−Cl bonds,[12] which are unlikely to form under hydrothermal conditions, because such bonds are hydrolytically unstable. A number of novel metal phosphate frameworks, including $AlPO_4$,[13−15] $ZrPO_4$,[4,15] $ZnPO_4$,[16,17] $GePO_4$,[18] $NiPO_4$,[19] and $GaPO_4$[20] materials have been synthesized successfully from ionic liquids or deep eutectic mixtures. Previously, we have shown how ionothermal synthesis can be performed in the zirconium phosphate system. We used deep eutectic solvents (DES),[4,15,21−23] consisting of urea or oxalic acid and quaternary ammonium salts. The structure-directing role of the quaternary ammonium cation could be observed in the oxalic-acid-based DES synthesis of ZrPOF-EA,[21] a novel open-framework zirconium phosphate synthesized in the presence of ethylammonium ions. The framework proved to have unusual 7-ring channels and displayed a gas adsorption selectivity for CO_2 over CH_4 that is significantly higher (adsorption ratio 17.3 at 1 bar) than that of typical 8-ring materials.

To the best of our knowledge, these ionic deep eutectic solvent syntheses are the only examples of syntheses of zirconium phosphate materials from ionic liquids. Therefore, we decided to explore the system further, using the ionic liquid *N*-ethylpyridinium (Epy) bromide as both solvent and template with the aim of synthesizing new zirconium phosphate materials. In this series of syntheses, a layered zirconium phosphate (denoted ZrPOF-Epy) was produced, and here we report its synthesis and structural characterization.

EXPERIMENTAL SECTION

Raw Chemicals. Zirconium(IV) oxychloride octahydrate ($ZrOCl_2 \cdot 8H_2O$, 99 wt %), orthophosphoric acid (H_3PO_4, 85 wt % in water), and hydrogen fluoride (HF, 40 wt % in water) were purchased from Aladdin Reagent Co. Ltd. (China). The ionic liquid *N*-ethylpyridinium bromide ([Epy]Br, 99 wt %) was purchased from Lanzhou Greenchem ILS, LICP, CAS, China.

Synthesis. In a typical synthesis of ZrPOF-Epy, a Teflon-lined autoclave (total volume 23 mL) was charged with [Epy]Br (3.7 g, 19.50 mmol), $ZrOCl_2 \cdot 8H_2O$ (250 mg, 0.76 mmol), H_3PO_4 (90 mg, 0.78 mmol), and HF (100 μL, 2.3 mmol). The autoclave was heated at 180 °C for 4 days and then cooled to room temperature. The solid product was recovered by filtration after the reaction mixture had been dissolved in distilled water. It was then washed thoroughly with alcohol and dried at room temperature.

Received: May 15, 2015
Published: August 3, 2015

ACS Publications © 2015 American Chemical Society

DOI: 10.1021/acs.inorgchem.5b01094
Inorg. Chem. 2015, 54, 7953−7958

Characterization. X-ray powder diffraction (XPD) patterns were recorded on a Rigaku Miniflex II X-ray diffractometer with Cu Kα radiation (λ = 1.5418 Å) in the 2θ range of 3−45° with a scan rate of 2°/min. Synchrotron X-ray powder diffraction data for the structure determination and refinement were collected on an as-synthesized sample of ZrPOF-Epy in a 0.3 mm capillary on the Materials Science beamline at the Swiss Light Source (wavelength 0.70822 Å, MYTHEN II detector) in Villigen, Switzerland.[24] CHN elemental analysis was carried out on an Elementar Vario EL analyzer. SEM images were obtained using a Hitachi S4800 scanning electron microscope. Thermogravimetric analysis was performed using a simultaneous thermal analyzer (SDT Q600 TGA/DSC, TA Instrument) in air with a heating rate of 10 °C/min. Solid state ^{13}C CP/MAS NMR measurement was performed on a Bruker Avance III 600 spectrometer at a resonance frequency of 150.9 MHz, and the chemical shifts were referenced externally to tetramethylsilane (TMS).

RESULTS

ZrPOF-Epy crystallized in the form of long flat needles, up to 1 μm in width and 10 μm in length (Figure 1). The synchrotron

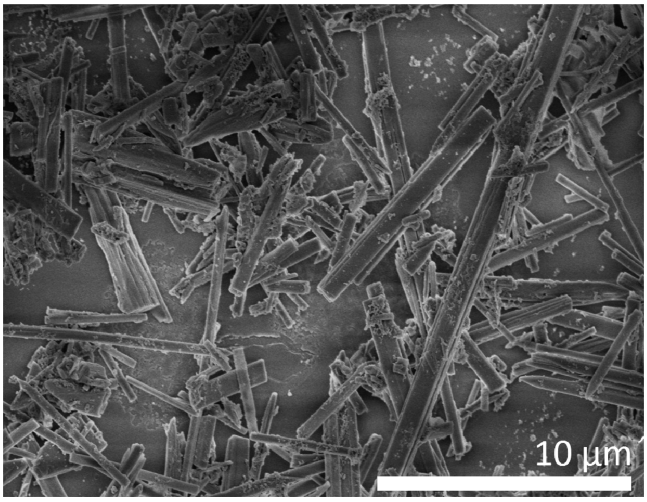

Figure 1. Scanning electron micrograph of the ZrPoF-Epy sample.

XPD data proved to be of very high quality, with sharp peaks and a maximum resolution of approximately 0.5 Å. The data were indexed with the routine implemented in Topas,[25,26] revealing a primitive monoclinic unit cell (extinction symbol $P12_11$; a = 6.6313 Å, b = 15.4064 Å, c = 11.9174 Å, β = 103.24°). The a parameter is similar to a typical Zr−O−P−O−Zr distance, and this gave us confidence that the cell was sensible. Reflection intensities were extracted in the highest possible symmetry, $P2_1/m$, using the Pawley peak-fitting routine[27] implemented in Topas. In view of the fact that Zr is a strong scatterer, we first tried to solve the structure using the powder charge-flipping algorithm (pCF)[28] implemented in Superflip.[29] Indeed, the structure could be solved in the space groups $P2$, $P2_1$, and $P2_1/m$ using default parameters. Most solutions generated by Superflip were similar. All Zr and P atoms, and most of the O atoms, were located directly from the electron density map, revealing a layered structure consisting of alternating ZrO_6 octahedra and PO_4 tetrahedra, a common arrangement in zirconium phosphates.

Missing O atoms were added in the expected locations, and Rietveld refinement[30] was initiated in the space group $P2_1/m$ using Topas. One O atom was found to make a particularly long bond to two Zr atoms (close to 2.1 Å) and was assigned as F. A difference Fourier map exposed some residual electron density between the layers, so to complete the structure, we applied a method that we have been using for locating the organic structure-directing agents (SDAs) in zeolites.[31−33] That is, a model of the Epy ion was generated and optimized using the energy minimization routine in Jmol.[34] It was then added to the structure as a rigid body, and its initial location and orientation were found by applying the simulated annealing routine in Topas, with the aim of using this as a starting point for refinement. However, it proved to be difficult to find a good position for the Epy ion, because it tended to settle on a point of 2-fold symmetry, resulting in a disordered arrangement. By reducing the symmetry to $P2_1$ and increasing the number of independent Epy ions to two, it was possible for the Epy ion to adopt two fully ordered positions.

Although most of the electron density should now be accounted for, the profile fit was still quite poor because of a problem with the peak shape. Closer inspection revealed shoulders on the peaks of the main phase. There was no indication that changing the unit cell or space group would index these shoulders, so we concluded that there was a small but significant amount of impurity in the sample that was hindering a good refinement.

We thought that the material could be partially dehydrated, giving rise to a dehydrated and hydrated phase with closely related structures. Therefore, we tried to hydrate the sample by leaving it in a desiccator with humid atmosphere for one month to ensure the sample would be fully hydrated. The sample was remeasured at the Materials Science beamline, but the shoulders were still present. Our next thought was to dehydrate the sample. This was done by attaching a filled capillary to a vacuum line and leaving it at room temperature for 30 min. While still under vacuum, the sample was heated to 100 °C at 5.0°/min in an oven and left for 1 h at that temperature. The capillary was sealed with a flame, and the sample remeasured. However, this still did not eliminate the shoulders. In the end, a new set of ZrPOF-Epy materials was synthesized under slightly different conditions (Table 1). The materials were measured once again, and although the diffraction patterns looked nearly identical to the previous ones, the shoulders were no longer present in the new samples.

The refinement was continued with the new data collected on ZrPOF-Epy (B1). The background was removed manually and adjusted during the course of the refinement. Distance and

Table 1. Synthetic Conditions Used to Prepare Different Samples of ZrPOF-Epy

sample name	ratio of the reactants[1]	synthetic conditions
A (original)	3.0HF:$ZrOCl_2$:1.5H_3PO_4:26[Epy]Br:14.6H_2O	180 °C, 4 days
B1	3.0HF:$ZrOCl_2$:1.0H_3PO_4:26[Epy]Br:14.1H_2O	180 °C, 4 days
B2	3.6HF:$ZrOCl_2$:1.0H_3PO_4:26[Epy]Br:15.1H_2O	180 °C, 4 days
B3	3.0HF:$ZrOCl_2$:0.7H_3PO_4:26[Epy]Br:13.8H_2O	180 °C, 4 days

[1]No extra water was added in these syntheses. The calculated amount of water comes from the aqueous HF and H_3PO_4 solutions and $ZrOCl_2\cdot 8H_2O$.

DOI: 10.1021/acs.inorgchem.5b01094
Inorg. Chem. 2015, 54, 7953−7958

angle restraints were set on all the ZrO_6 and ZrO_5F octahedra and PO_4 tetrahedra. All atoms were refined with isotropic displacement parameters, using a common value for each atom type. Line broadening was refined using an anisotropic model,[35] and peak asymmetry was described by applying a model for the axial divergence of the beam.

Although the refinement converged well, the intermolecular distances between the ethyl group of one of the Epy ions and the $ZrPO_4$ layers were too short (<2.4 Å). Therefore, the rigid-body Epy models were converted to restrained ones to allow them more flexibility. Although this improved the profile fit, it did not eliminate the short distances. The molecule was rotated to try several different directions for the ethyl group, but none resulted in chemically sensible intermolecular distances. Furthermore, the occupancies of the two Epy ions each refined to approximately 0.8. This prompted the question as to whether it was actually Epy incorporated in the material. The number of electrons for an Epy ion with an occupancy of 0.8 corresponds very well to that for a fully occupied pyridinium (py) ion. Without the ethyl group of Epy, a py ion would fit perfectly between the $ZrPO_4$ layers. Several models with a number of combinations of py, Epy, and water were investigated in an attempt to get a good model for the electron density between the layers. The model with one py and one Epy ion resulted in the best profile fit and made the most chemical sense.

To verify our suspicion that both py and Epy ions might be present, we turned to other methods to characterize the material. The first piece of evidence in favor of a mixed py/Epy incorporation was the elemental analysis. The C:N ratio of 6.5 (Table 2) lies between the values expected for py (5.0) and Epy (7.0). The ^{13}C MAS NMR spectrum of ZrPOF-Epy (Figure 2) has 2 signals at low ppm, which confirm the inclusion of Epy. However, at higher ppm, 4 signals are clearly visible, instead of the 3 expected for Epy alone, but the assignment of the peaks is ambiguous. This extra signal may be caused by the presence of a second moiety, such as py. The other possibility is that these shifts are caused by the confinement effect, which at the very least confirms the presence of two independent organic species in the sample. The TGA analysis (Figure 3) shows a region of about 5% weight loss up to 270 °C, which corresponds to water. We considered a model with water in place of one of the organic species, but the XPD profile fit was significantly worse, and the water molecules seemed to arrange themselves in a ring with short O−O distances reminiscent of a cycloalkane, so this model was discarded. The next region in the TGA between 270° to 450° shows a weight loss of approximately 23%. This corresponds quite well to the amount of mixed py/Epy found between the layers in the Rietveld refinement (20% of the total mass).

Table 2. Elemental Analysis of ZrPOF-Epy

	wt %	molar composition
C	15.62%	6.5
H	1.98%	9.7
N	2.86%	1

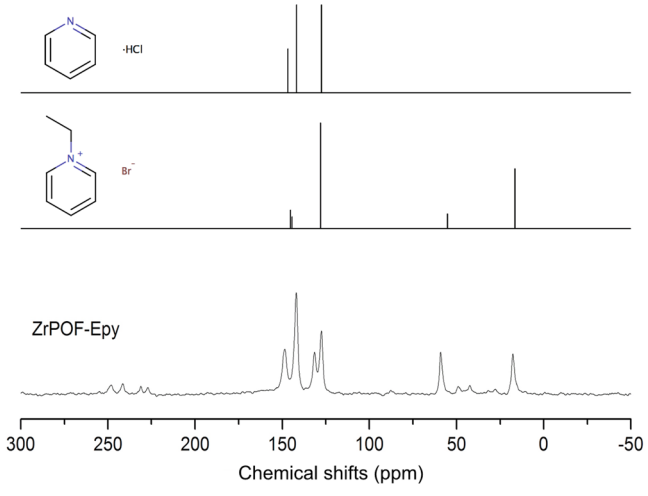

Figure 2. ^{13}C CP/MAS NMR spectrum of ZrPOF-Epy (bottom) with the liquid NMR spectra for [Epy]Br and pyCl for comparison.

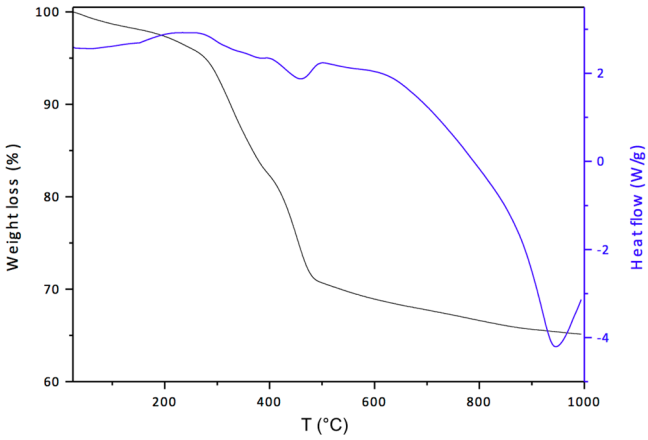

Figure 3. Thermogravimetric analysis curve for ZrPOF-Epy.

Considering everything together, we believe that both py and Epy ions are present between the $ZrPO_4$ layers. Hydrogen atoms were added to the py and Epy ions at their expected positions, and the occupancies for py and Epy refined to 0.89(1) and 0.81(1), respectively. The position of the N atom in the py molecule was ambiguous, due to the lack of contrast between N and C in XPD, so it was assigned arbitrarily. The final structure converged with the agreement values R_I = 0.083 and R_{wp} = 0.136 (R_{exp} = 0.007) (Table 3). The profile fit is shown in Figure 4.

The diffraction patterns measured as a function of temperature (Figure 5) show that ZrPOF-Epy does not possess high thermal stability. At 300 °C, most of the material has lost any long-range order. The temperature is significantly lower than reported for zirconium phosphates with 3D connected frameworks,[21,22] which are stable up to 410 °C.

DISCUSSION

The structure of ZrPOF-Epy consists of alternating corner sharing ZrO_6/ZrO_5F octahedra and PO_4 tetrahedra, forming layers in the *xy* plane (Figure 6). Three independent tetrahedra and three independent octahedra form the basic building unit (Figure 7), which in turn forms chains along the *y* axis, where each unit is rotated by 180° around the *y* axis with respect to its neighbor. These chains are stacked along the *x* axis to form an undulating ZrPOF layer. Each P tetrahedron is connected to 4 Zr octahedra via O atoms. Each ZrO_6/ZrO_5F octahedron is, in turn, connected to 4 P tetrahedra. The two independent ZrO_5F octahedra are further connected to one another via a bridging F

DOI: 10.1021/acs.inorgchem.5b01094
Inorg. Chem. 2015, 54, 7953−7958

Table 3. Crystallographic Details for ZrPOF-Epy

refined chemical composition	$\mid(C_5H_6N^+)_{1.77}(C_7H_{10}N^+)_{1.62}\mid [Zr_6P_6O_{28}F_2(H_2O)_4]$
space group	$P2_1$
a (Å)	6.6331(1)
b (Å)	15.4171(1)
c (Å)	11.9417(1)
β (deg)	103.34(1)
V (Å^3)	1188.2
2θ range (deg)	2.0−45.0
λ (Å)	0.70822(1)
R_I	0.083
R_{wp}	0.136
R_{exp}	0.007
GoF	18.7
observations	11316
reflections	1696
parameters	187
geometric restraints	122
Zr−O/F 2.10(1) Å	18
P−O 1.55(1) Å	12
O/F−Zr−O/F 90.0(8)°/180.0(8)°	45
O−P−O 109.5(8)°	18
C−C/N 1.337(7)−1.513(7) Å[42]	14
C/N−N/C−C 120.0(5)°/109.5(5)°	15

atom. The remaining four O atoms in the basic building unit are terminal and protrude into the space between the layers. From charge balance arguments, these are probably water molecules coordinated to the Zr in the layer. The structure of ZrPOF-Epy is quite distinct from that of the classical layered zirconium phosphate material α-$ZrPO_4$,[36] even though both

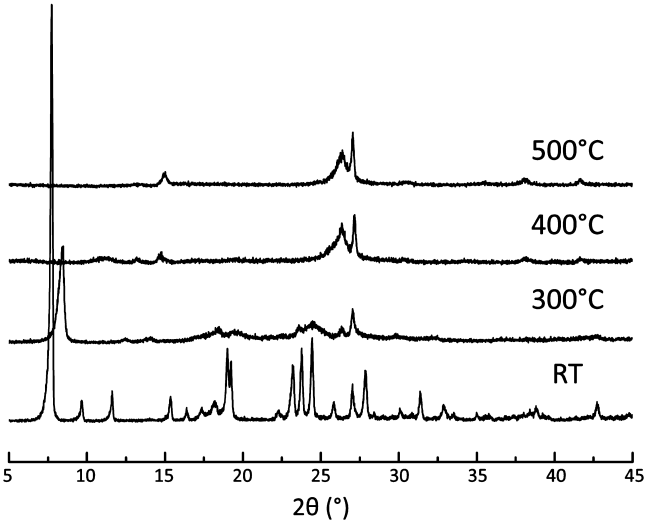

Figure 5. XPD patterns of ZrPO-Epy after heat treatment in air at different temperatures.

consist of layers of corner-sharing Zr octahedra and P tetrahedra. The main difference is that all the P atoms in ZrPOF-Epy are 4-connected to Zr atoms via O atom bridges, while those in α-$ZrPO_4$ are all 3-connected with the fourth O atom terminating the layer. In ZrPOF-Epy, the terminal O atoms are connected exclusively to Zr. This arrangement leads to undulating ZrPOF layers with P polyhedra in the middle and Zr polyhedra on the outside, while the layers in α-$ZrPO_4$ are flat with the Zr and P polyhedra reversed.

The ZrPOF layers in ZrPOF-Epy are separated by the organic cations, which are neatly intercalated between the

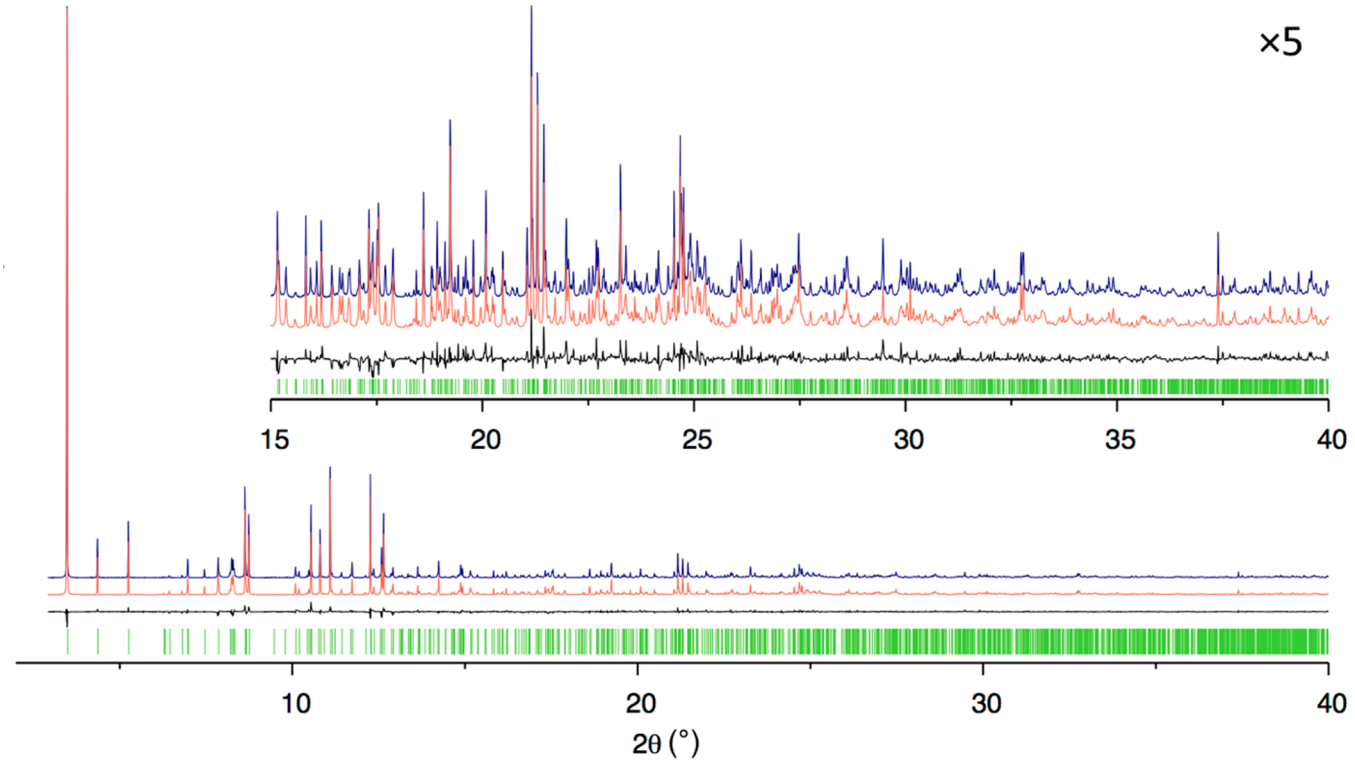

Figure 4. Observed (top), calculated (middle), and difference (bottom) profiles for the Rietveld refinement of ZrPOF-Epy. Vertical bars indicate the positions where reflections are expected. The intensity of the inset has been increased by a factor of 5 to show more detail.

DOI: 10.1021/acs.inorgchem.5b01094
Inorg. Chem. 2015, 54, 7953−7958

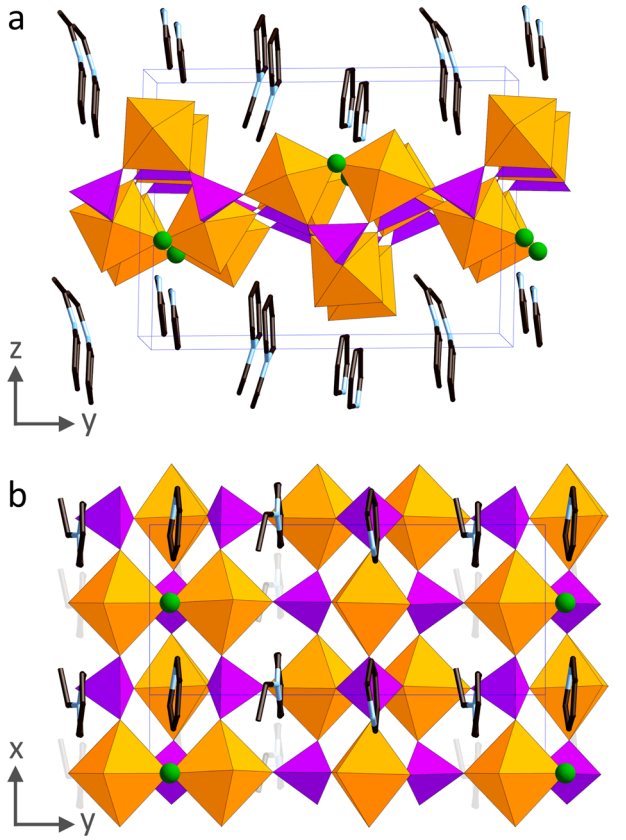

Figure 6. Views of the ZrPOF-Epy crystal structure along the (a) [100] and (b) [001] directions showing the ZrO_6/ZrO_5F octahedra (orange), PO_4 tetrahedra (purple), the F atom (green) and the py/Epy cations.

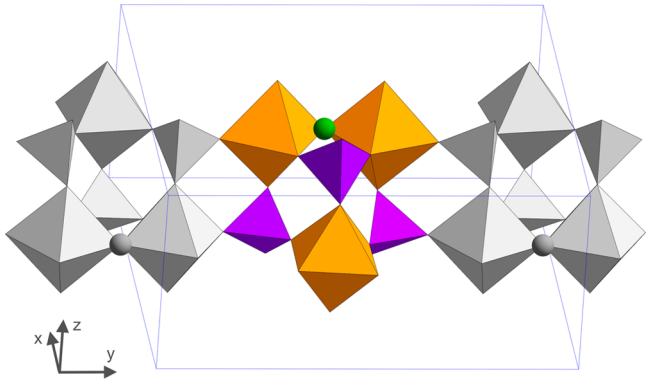

Figure 7. Projection of the ZrPOF-Epy crystal structure showing the basic building unit (colored). It is related to the neighboring units (in gray) via a 2_1 rotation axis along *y*.

terminal O atoms. The pyridine rings of the cations are stacked along the *y* axis, at a typical distance of about 3.8 Å. The closest distances between the SDAs and the framework are 3.090(6) between C17 and O17, and 3.099(9) between N23 and O15.

Although it was surprising to find py included between the layers of ZrPOF-Epy, partial decomposition of Epy is not unusual. *N*-alkylpyridinium cations can be converted to pyridinium cations under certain conditions.[37] In the ionothermal aluminophosphate zeotype synthesis from 1-ethylpyridinium bromide,[38,39] the breakdown of Epy to py has been observed and confirmed by 1H-NMR spectra. In the presence of fluoride, some of the *N*-alkyl bonds in imidazolium cations can also be broken and reformed under ionothermal synthesis conditions.[40] Other investigations have shown that ethylenediamine could be partially converted to ammonium in a mixture of H_3PO_4−(*i*-PrO)$_3$Al−ethylenediamine−ethylene glycol−water, resulting in the formation of a chain aluminophosphate with a combination of the ammonium cations and ethylenediamine as templating agents.[41]

CONCLUSION

We have described the structure of a new layered zirconium phosphate that was synthesized ionothermally using Epy as a structure directing agent. The structure was elucidated using XPD data and revealed that not only Epy but also py had been occluded between the layers. We expect that the Epy decomposed as a result of the harsh synthesis conditions. It was exciting that we were able to reach this conclusion on the basis of the XPD data alone. Structure refinement with XPD data is not generally considered to be very sensitive to such information, but in this case, the unexpected result was quite clear. The result could be corroborated using several complementary methods.

ASSOCIATED CONTENT

Supporting Information

The Supporting Information is available free of charge on the ACS Publications website at DOI: 10.1021/acs.inorgchem.5b01094.

Crystallographic information for ZrPOF-Epy (CIF)

AUTHOR INFORMATION

Corresponding Authors

*E-mail: liulei@tyut.edu.cn.
*E-mail: mccusker@mat.ethz.ch.

Author Contributions

The manuscript was written through contributions of all authors. All authors have given approval to the final version of the manuscript.

Notes

The authors declare no competing financial interest.

ACKNOWLEDGMENTS

We thank Nicola Casati and Antonio Cervellino at the Materials Science beamline at the SLS in Villigen, Switzerland, for their assistance with the powder diffraction measurements and Ana Pinar at ETH Zurich for dehydrating the sample. Funding from the Swiss National Science Foundation is gratefully acknowledged. The Chinese group was financially supported by the National Natural Science Foundation (Grants 21276174 and 21322608), Shanxi Province Science Foundation for Youths (Grant 2014021005), and a Foundation for the Author of National Excellent Doctoral Dissertation of PR China (Grant 201350).

REFERENCES

(1) Murugavel, R.; Choudhury, A.; Walawalkar, M. G.; Pothiraja, R.; Rao, C. N. R. *Chem. Rev.* **2008**, *108*, 3549−3655.
(2) Vivani, R.; Alberti, G.; Costantino, F.; Nocchetti, M. *Microporous Mesoporous Mater.* **2008**, *107*, 58−70.
(3) Clearfield, A. *Mater. Chem. Phys.* **1993**, 35, 257−263.
(4) Liu, L.; Li, Y.; Wei, H.; Dong, M.; Wang, J.; Slawin, A. M. Z.; Li, J.; Dong, J.; Morris, R. E. *Angew. Chem.* **2009**, *121*, 2240−2243.

DOI: 10.1021/acs.inorgchem.5b01094
Inorg. Chem. 2015, 54, 7953−7958

(5) Du, Y.; Pan, Q.; Li, J.; Yu, J.; Xu, R. *Inorg. Chem.* **2007**, *46*, 5847−5851.
(6) Liu, L.; Li, J.; Dong, J.; Šišak, D.; Baerlocher, C.; McCusker, L. B. *Inorg. Chem.* **2009**, *48*, 8947−8954.
(7) Dong, J.; Liu, L.; Li, J.; Li, Y.; Baerlocher, C.; McCusker, L. B. *Microporous Mesoporous Mater.* **2007**, *104*, 185−191.
(8) Zhang, X.; Xu, H.; Zuo, Z.; Lin, Z.; Ferdov, S.; Dong, J. *ACS Appl. Mater. Interfaces* **2013**, *5*, 7989−7994.
(9) Cooper, E. R.; Andrews, C. D.; Wheatley, P. S.; Webb, P. B.; Wormald, P.; Morris, R. E. *Nature* **2004**, *430*, 1012−1016.
(10) Parnham, E. R.; Morris, R. E. *Acc. Chem. Res.* **2007**, *40*, 1005−1013.
(11) Morris, R. E. *Chem. Commun.* **2009**, 2990−2998.
(12) Drylie, E. A.; Wragg, D. S.; Parnham, E. R.; Wheatley, P. S.; Slawin, A. M. Z.; Warren, J. E.; Morris, R. E. *Angew. Chem., Int. Ed.* **2007**, *46*, 7839−7843.
(13) Xing, H.; Li, J.; Yan, W.; Chen, P.; Jin, Z.; Yu, J.; Dai, S.; Xu, R. *Chem. Mater.* **2008**, *20*, 4179−4181.
(14) Wei, Y.; Tian, Z.; Gies, H.; Xu, R.; Ma, H.; Pei, R.; Zhang, W.; Xu, Y.; Wang, L.; Li, K.; Wang, B.; Wen, G.; Lin, L. *Angew. Chem., Int. Ed.* **2010**, *49*, 5367−5370.
(15) Liu, L.; Chen, Z.-F.; Wei, H.-B.; Li, Y.; Fu, Y.-C.; Xu, H.; Li, J.-P.; Slawin, A. M. Z.; Dong, J.-X. *Inorg. Chem.* **2010**, *49*, 8270−8275.
(16) Liu, L.; Ferdov, S.; Coelho, C.; Kong, Y.; Mafra, L.; Li, J. P.; Dong, J. X.; Kolitsch, U.; Sá Ferreira, R. A.; Tillmanns, E.; Rocha, J.; Lin, Z. *Inorg. Chem.* **2009**, *48*, 4598−4600.
(17) Jhang, P.-C.; Chuang, N.-T.; Wang, S.-L. *Angew. Chem., Int. Ed.* **2010**, *49*, 4200−4204.
(18) Wang, W.; Li, Y.; Liu, L.; Dong, J. *Dalton T.* **2012**, *41*, 10511−10513.
(19) Xing, H.; Yang, W.; Su, T.; Li, Y.; Xu, J.; Nakano, T.; Yu, J.; Xu, R. *Angew. Chem.* **2010**, *122*, 2378−2381.
(20) Lohmeier, S.-J.; Wiebcke, M.; Behrens, P. *Z. Anorg. Allg. Chem.* **2008**, *634*, 147−152.
(21) Liu, L.; Yang, J.; Li, J.; Dong, J.; Šišak, D.; Luzzatto, M.; McCusker, L. *Angew. Chem., Int. Ed.* **2011**, *50*, 8139−8142.
(22) Kubli, M.; Šišak, D.; Baerlocher, C.; McCusker, L. B.; Liu, L.; Yang, J.; Li, J.; Dong, J. *Microporous Mesoporous Mater.* **2012**, *164*, 82−87.
(23) Wang, W.; Liu, L.; Yang, J.; Li, S.; Li, J.; Dong, J. *Dalton T.* **2012**, *41*, 12915−12919.
(24) Bergamaschi, A.; Cervellino, A.; Dinapoli, R.; Gozzo, F.; Henrich, B.; Johnson, I.; Kraft, P.; Mozzanica, A.; Schmitt, B.; Shi, X. *J. Synchrotron Radiat.* **2010**, *17*, 653−668.
(25) Coelho, A. A. *J. Appl. Crystallogr.* **2003**, *36*, 86−95.
(26) Coelho, A. A. TOPAS-ACADEMIC v5.0, 2012.
(27) Pawley, G. S. *J. Appl. Crystallogr.* **1981**, *14*, 357−361.
(28) Baerlocher, C.; McCusker, L. B.; Palatinus, L. *Z. Kristallogr. Cryst. Mater.* **2007**, *222*, 47−53.
(29) Palatinus, L.; Chapuis, G. *J. Appl. Crystallogr.* **2007**, *40*, 786−790.
(30) Rietveld, H. M. *J. Appl. Crystallogr.* **1969**, *2*, 65−71.
(31) Smeets, S.; Xie, D.; McCusker, L. B.; Baerlocher, C.; Zones, S. I.; Thompson, J. A.; Lacheen, H. S.; Huang, H.-M. *Chem. Mater.* **2014**, *26*, 3909−3913.
(32) Smeets, S.; Xie, D.; Baerlocher, C.; McCusker, L. B.; Wan, W.; Zou, X.; Zones, S. I. *Angew. Chem.* **2014**, *126*, 10566−10570.
(33) Smeets, S.; McCusker, L. B.; Baerlocher, C.; Xie, D.; Chen, C. Y.; Zones, S. I. *J. Am. Chem. Soc.* **2015**, *137*, 2015−2020.
(34) Hanson, R. M. *J. Appl. Crystallogr.* **2010**, *43*, 1250−1260.
(35) Stephens, P. W. *J. Appl. Crystallogr.* **1999**, *32*, 281−289.
(36) Clearfield, A.; Smith, G. D. *Inorg. Chem.* **1969**, *8*, 431−436.
(37) Katritzky, A. R.; Watson, C. H.; Dega-Szafran, Z.; Eyler, J. R. *J. Am. Chem. Soc.* **1990**, *112*, 2479−2484.
(38) Wragg, D. S.; Slawin, A. M.; Morris, R. E. *Solid State Sci.* **2009**, *11*, 411−416.
(39) Wragg, D. S.; Fullerton, G. M.; Byrne, P. J.; Slawin, A. M.; Warren, J. E.; Teat, S. J.; Morris, R. E. *Dalton T.* **2011**, *40*, 4926−4932.
(40) Parnham, E. R.; Morris, R. E. *Chem. Mater.* **2006**, *18*, 4882−4887.
(41) Gao, Q.; Chen, J.; Li, S.; Xu, R.; Thomas, J. M.; Light, M.; Hursthouse, M. B. *J. Solid State Chem.* **1996**, *127*, 145−150.
(42) Allen, F.; Watson, D.; Brammer, L.; Orpen, A.; Taylor, R. In *International Tables for Crystallography Vol. C: Mathematical, Physical and Chemical Tables*; Springer: New York, 2004; pp 790−811.

DOI: 10.1021/acs.inorgchem.5b01094
Inorg. Chem. 2015, 54, 7953−7958